INTEGRATED LOCAL AND REGIONAL PHOTOGEOLOGIC MAPPING OF NEUKUM CRATER AND EASTERN NOACHIS TERRA, MARS H. Bernhardt and D. A. Williams. School of Earth and Space Exploration, Arizona State University, Tempe, USA (h.bernhardt@asu.edu).

Introduction: Integrating local-scale with regional to continental-scale photogeologic maps allows extrapolating the geomorphologic inventory of large areas at a detail beyond regional-scale datasets. As part of an upcoming, comprehensive investigation of the region as well as a tribute to the late Gerhard Neukum, we present a case study based on Neukum crater, which we employ as representative local morphologic ensemble for surrounding eastern Noachis Terra. Neukum is a 102 km large crater in eastern Noachis Terra, a ~1.8 x 10^6 km^2 large part of the cratered highlands west of the Hellas basin in the southern hemisphere of Mars. Eastern Noachis Terra is the type area of the middle Noachian stratigraphic system [1-3], hosts several exposures of "felsic/anorthosite-like/plagioclase-rich" signatures associated with infrared-dark areas [4,5], and preserved the effects of the Hellas impact event (ejecta, secondaries, impact/related tectonics) because of a general lack of volcanic and fluvial overprint [e.g., 6-8]. Thus, it is a key region to better understand the martian impact chronology, the geologic and climatic effects of large impact events on the planet's history [e.g., 9], as well as early crustal evolution. However, despite some local, isolated investigations, no comprehensive analysis of the region has been conducted yet.

Data: We used mid-infrared data from version 12 of the Thermal Emission Imaging System (THEMIS) Daytime global mosaic (100 m/px) [10] as well as High Resolution Stereo Camera images (HRSC; 12.5-50 m/px) [11,12] as basemap for our regional mapping (1:1,000,000). To assess thermophysical properties of the surface, we also used the global thermal inertia mosaic based on THEMIS-IR [13]. Our local map (Fig. 1) is based on images by the Context Camera (CTX; ~6 m/px) [14-16]. Stereographic digital terrain models (DTMs; 50 m/px) based on HRSC images [17] covering Neukum crater were used to improve topographic information, which enabled better resolved stratigraphic observations. For the remainder of eastern Noachis Terra, the global DTM by the Mars Orbiter Laser Altimeter (MOLA) with a horizontal resolution of 463 m/px served as topographic basemap [18,19]. Further datasets (HiRISE, CRISM, and OMEGA) will be used for detailed unit interpretations in our final publication.

Technique: We used standard symbology defined by the US Geological Survey and employed the general techniques for planetary mapping as outlined by [20-22]. While contact classification is ongoing for the regional map, we defined standard contact types (certain, approximate, inferred, covered) for the local map. In addition to relative dating via stratigraphic analyses, we have derived absolute model ages by measuring crater-size frequency distributions (CSFD) on suitable local map units using techniques described in [23,24], with the aid of CraterTools in ArcMap [25] and CraterStats for plotting and fitting the distributions [26]. For the regional map, CSFD measurements are ongoing and several different production and chronology functions [27-30] will be used to derive model ages in order to ensure comparability with previous investigations.

Preliminary results and discussion: Integrated local and regional observations showed that Neukum crater's geomorphology is representative for eastern Noachis Terra (overall crater degradation stage, relatively smooth infill dissected by 10s of km-scale pits, infrared-dark zones on crater floor, furrowed inner crater wall, dark dune field). The IR-dark zones, previously associated with "felsic" or plagioclase-rich signatures in several craters of northeastern Noachis Terra [4,5], do not correlate well with CTX-based photogeologic units. Instead, HiRISE and CRISM observations show Neukum's larger pit, which dissects an IR-dark zone, to expose bright, layered, smectite-bearing material. We interpret the bright, smectite-bearing material as hydrothermal alteration product of the "felsic"/plagioclase-rich outcrops. As the often terraced walls and floors of all the crater floor pits of eastern Noachis Terra expose up to ~250 m of this bright, layered material, we submit that hydrothermal alteration followed or accompanied the emplacement of plagioclase-rich volcanic material (possibly via fractional crystallization of basalt [4,5]) and persisted over extended time spans in a large area. Lastly, despite having similar combined volumes (~1,600 km^3), the bright, smectite-exposing pits of eastern Noachis Terra are unlikely to be significant sources of the dune fields of the region (as suggested by [31]), which completely lack such characteristics, but are very dark and show mafic signatures.

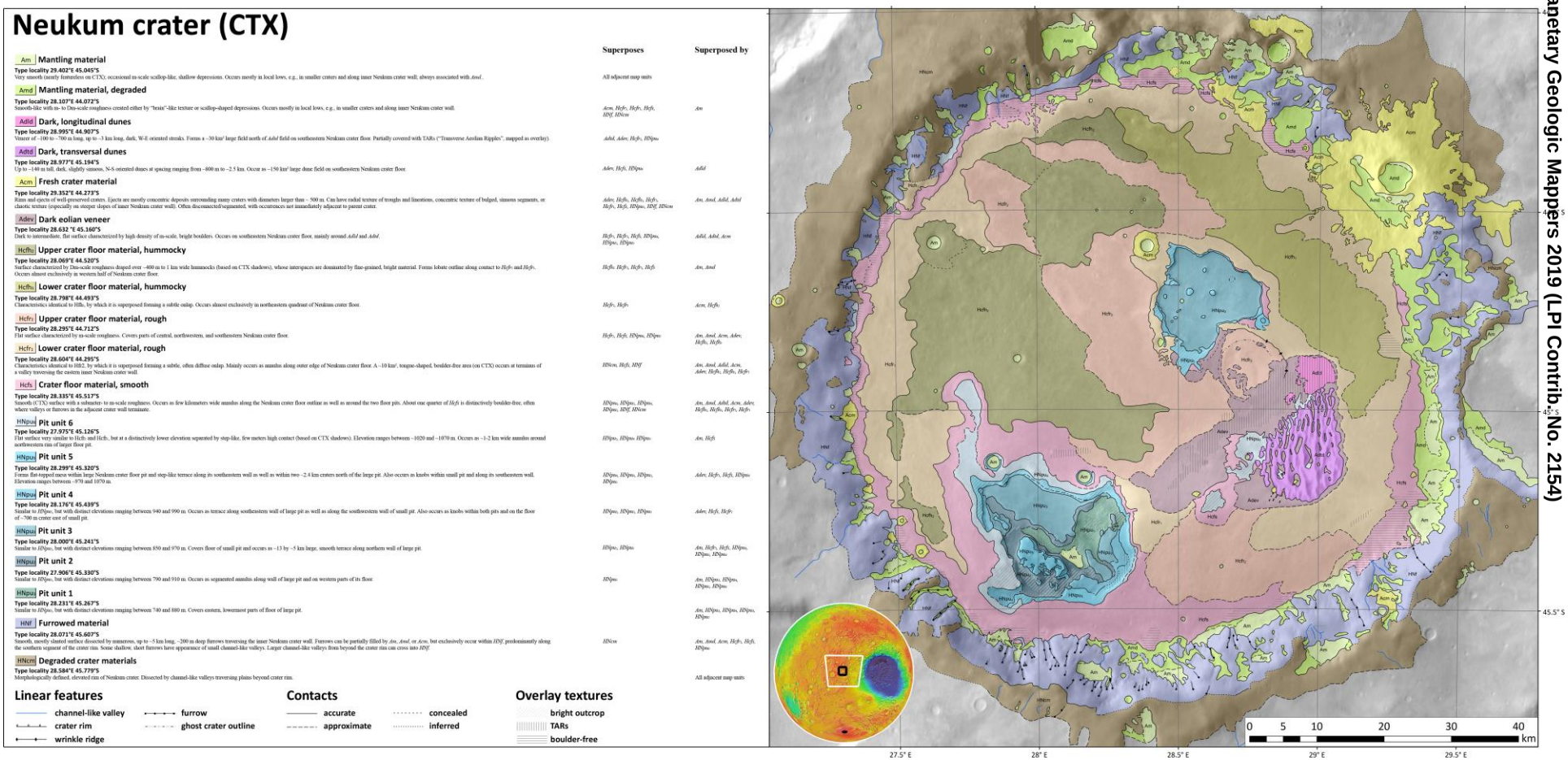

Figure 1: Our local-scale map of Neukum crater along with a description of map units and stratigraphic observations (orthographic projection centered at crater center; location indicated by black box on global overview). While local mapping is based on CTX data, the product is shown with a THEMIS-IR day background for better visibility. This local-scale map complements our ongoing regional-scale mapping of surrounding eastern Noachis Terra (not shown in this abstract; outlines indicated by white box on global overview).

References: [1] Peterson, J. E. (1977). *USGS* IMAP 910. [2] Scott, D. H., & Carr, M. H. (1978). *USGS* IMAP 1083. [3] Tanaka, K. L. et al. (1988) *LPSC Proceedings* (A89-10851 01-91). [4] Wray, J. J. et al. (2013). *Nature Geoscience*, 6(12), 1013–1017. [5] Rogers, A. D., & Nekvasil, H. (2015). *GRL*, 42(8), 2619–2626. [6] Morrison, S. J., & Frey, H. V. (2007). *LPSC* 1355. [7] Tanaka, K. L. et al. (2014). *USGS* IMAP 3292. [8] Hynek, B. M., et al. (2010). *JGR: Planets*, 115(E9), 1–14. [9] Segura, T. L. et al. (2002). *Science*, 298(5600), 1977–1980. [10] Christensen, P. R. et al. (2004) *Space Sci. Rev.*, *110*(1/2), 85–130. [11] Neukum, G., & Jaumann, R. (2004) *Mars Express: The Scientific Payload*, 1–19. [12] Jaumann, R. et al. (2007) *PSS*, *55*(7-8), 928–952. [13] Christensen, P. R. et al. (2013) *LPSC*, 2822. [14] Malin, M. C. et al. (2007) *JGR*, *112*(E5), E05S04. [15] McEwen, A. S. (2006) *JGR*, *112*. [16] Delamere, W. A. et al. (2010) *Icarus*, *205*(1), 38–52. [17] Gwinner, K. et al. (2009) *Photogrammetric Engineering & Remote Sensing*, *75*(9), 1127–1142. [18] Smith, M. D. et al. (2001) *JGR*, *106*(E10), 23689. [19] Zuber, M. T., & Smith, M. D. (1992) *JGR*, *97*(92), 7781–7797. [20] Wilhelms, D. E. (1990) Geologic Mapping. In *Planetary Mapping* (p. 312). [21] Tanaka, K. L. et al. (2009) *PSS*, *57*(5-6), 510–532. [22] Skinner at el. (2018), USGS Planetary Geologic Mapping Protocol. [23] Neukum, G. (1983) Habil. thesis, U. of Munich. [24] Neukum, G. et al. (2001) *SSR*, *96*, 55-86. [25] Kneissl, T. et al. (2012) *PSS*, *59*, 1243-1254. [26] Michael, G. and Neukum, G. (2010) *EPSL*, *294*, 223-229. [27] Ivanov, B. A. (2001). *SSR*, *96*(1-4), 87–104. [28] Hartmann & Neukum (2001), *SSR*, *96*, 165-194, [29] Hartmann & Daubar (2017), *MPS*, *52*, 493-510, [30] Hartmann (2005), *Icarus*, *174*, 294-320. [31] Fenton, L. K. (2005). *JGR*, 110(E11), E11004.